Myotonic Dystrophy Protein Kinase Domains Mediate Localization, Oligomerization, Novel Catalytic Activity, and Autoinhibition†

Erik W. Bush, Steve M. Helmke, Richard A. Birnbaum, and M. Benjamin Perryman*

Division of Cardiology, Department of Medicine, University of Colorado Health Sciences Center, Denver, Colorado 80262

Received September 14, 1999; Revised Manuscript Received May 9, 2000

ABSTRACT: Human myotonic dystrophy protein kinase (DMPK) is a member of a novel class of multidomain protein kinases that regulate cell size and shape in a variety of organisms. However, little is currently known about the general properties of DMPK including domain function, substrate specificity, and potential mechanisms of regulation. Two forms of the kinase are expressed in muscle, DMPK-1 and DMPK-2. We demonstrate that the larger DMPK-1 form (the primary translation product) is proteolytically cleaved near the carboxy terminus to generate the smaller DMPK-2 form. We further demonstrate that the coiled-coil domain is required for DMPK oligomerization; coiled-coil mediated oligomerization also correlated with enhanced catalytic activity. DMPK was found to exhibit a novel catalytic activity similar to, but distinct from, related protein kinases such as protein kinase C and A, and the Rho kinases. We observed that recombinant DMPK-1 exhibits low activity, whereas the activity of carboxy-terminally truncated DMPK is increased approximately 3-fold. The inhibitory activity of the full-length kinase was mapped to what appears to be a pseudosubstrate autoinhibitory domain at the extreme carboxy terminus of DMPK. To date, endogenous activators of DMPK are unknown; however, we observed that DMPK purified from cells exposed to the G protein activator GTP-γ-S exhibited an approximately 2-fold increase in activity. These results suggest a general model of DMPK regulation with two main regulatory branches: short-term activation of the kinase in response to G protein second messengers and long-term activation as a result of proteolysis.

Myotonic dystrophy (DM)[1] is an autosomal dominant, variably penetrant neuromuscular disorder affecting approximately 1 in 8000 individuals. Affected individuals display a wide range of symptoms including myotonia, skeletal muscle weakness and wasting, cardiac conduction abnormalities, and cataracts (for review, see ref *1*). Cloning of the DM locus revealed the underlying defect, an unstable CTG triplet repeat within the 3′ untranslated region of a gene for a novel protein kinase, myotonic dystrophy protein kinase (DMPK) (*2*−*5*). Despite cloning of the locus, the complex disease phenotype of DM has proven difficult to interpret, and the role of DMPK in the pathogenesis of DM remains unclear (summarized in ref *6*). The DMPK locus encodes a 629 amino acid multidomain protein, most abundant in skeletal and cardiac muscle, where it is localized to the neuromuscular junction and the intercalated disk, respectively (*7*−*9*). In vivo functions and modes of regulation of this kinase are currently unknown, but this localization suggests that this novel kinase is likely to function as a component of a previously uncharacterized signal transduction pathway in these tissues. Predicted DMPK domains include an N-terminal leucine-rich region (LR), a serine/threonine kinase catalytic domain, and C-terminal coiled-coil (CC) and membrane association (MA) domains (Figure 1). The membrane association domain is required for peripheral membrane association of the kinase (*10*), but the functions of other domains have not been determined.

Antibodies raised against various epitopes within DMPK have been used to demonstrate that two forms of the kinase are present in muscle (*7*−*10*), but the origin of these forms, their relationship to one another, and the functional differences between forms are unknown. The two DMPK forms differ in apparent molecular mass by approximately 8 kDa (*7, 8, 10*). We have designated the higher mass form as DMPK-1 and the smaller form as DMPK-2. Both forms are produced in mammalian cells transfected with a single DMPK cDNA construct, suggesting that one form is derived from the other by a posttranslational modification (*7*). In the current study, we utilized in vitro expressed DMPK and endogenous DMPK in tissue extracts to examine the relationship between DMPK-1 and DMPK-2. We demonstrate that the primary translation product is the larger form DMPK-1, which migrates anomalously in SDS−PAGE. Full-length membrane-associated DMPK-1 was found to be

† Supported by NIH Grant 1RO1HL50715, a grant from The Muscular Dystrophy Association, and a grant from the American Heart Association Desert Mountain Affiliate.

* Corresponding author: Division of Cardiology, Campus Box B139, University of Colorado Health Sciences Center, 4200 E. Ninth Ave., Denver, CO 80262. Telephone (303) 315-3259; fax: (303) 315-3261; e-mail: benjamin.perryman@UCHSC.edu.

[1] Abbreviations used are: DM, myotonic dystrophy; DMPK, myotonic dystrophy protein kinase; PKC, protein kinase C; PKA, protein kinase A; MLCK, myosin light-chain kinase; CaMK, calcium/calmodulin-dependent protein kinase; EGFR, epidermal growth factor receptor; PAGE, polyacrylamide gel electrophoresis; HA, hemagglutinin; AEBSF, 4-(2-aminoethyl)benzenesulfonyl fluoride; IPTG, isopropyl thio-β-D-galactoside; DTT, dithiothreitol; TX100, Triton X-100; TBS, Tris-buffered saline; BSA, bovine serum albumin; HRP, horseradish peroxidase; DMEM, Dulbecco's modified Eagle's medium; GST, glutathione *S*-transferase; GTP-γ-S, guanosine 5′-(3-*O*-thio)triphosphate.

10.1021/bi992142f CCC: $19.00
Published on Web 06/27/2000

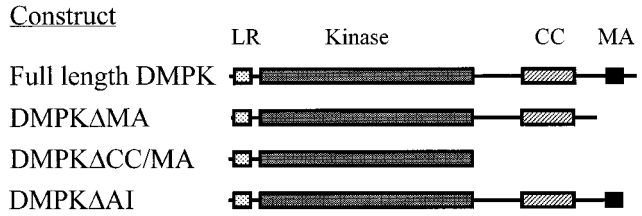

FIGURE 1: DMPK domains and cDNA constructs. Full-length DMPK domains include an amino-terminal leucine-rich region (LR), a serine/threonine protein kinase catalytic domain, a coiled-coil (CC), and a membrane association domain (MA). Domain-deleted cDNA constructs used in this study include DMPKΔMA (lacking sequences C-terminal to the coiled-coil, residues 550−629), DMPKΔCC/MA (lacking sequences C-terminal to the kinase domain, residues 378−629), and DMPKΔAI (lacking sequences C-terminal to the membrane association domain, residues 614−629). To facilitate immunoprecipitation, cDNA constructs were modified to encode a small N-terminal c-myc or hemagglutinin (HA) epitope tag.

converted into soluble DMPK-2 by a proteolytic cleavage that removes the C-terminal hydrophobic membrane association domain.

DMPK was originally described as most closely related to PKA and PKC, but the recent cloning of a number of kinases has revealed that DMPK is a member of an orthologous family of multidomain kinases (*11*). An unusual distinguishing feature of all metazoan members of the DMPK family is a coiled-coil domain, a helical interaction motif that mediates homo- or heterooligomerization of proteins (*12*). A recently characterized *Arabidopsis thaliana* gene, TOUSLED, encodes a nuclear serine/threonine kinase that requires a coiled-coil domain for oligomerization and enzymatic activity (*13*), raising the possibility that kinase activity can be regulated by coiled-coil-mediated oligomerization. Gel-filtration of in vitro expressed DMPK forms demonstrated that DMPK lacking both coiled-coil and membrane association domains exists as a monomer. Addition of the coiled-coil domain caused DMPK to elute as a much higher than predicted molecular weight species, consistent with the formation of oligomers.

Basal catalytic activity of full-length and truncated DMPK was examined by expression in mammalian cell culture followed by immunoprecipitation kinase assays. Oligomeric DMPK lacking the membrane association domain exhibited approximately 3-fold greater activity than monomeric DMPK lacking both coiled-coil and membrane association domains, indicating that enhanced kinase activity correlates with the ability to oligomerize. Interestingly, full-length DMPK exhibited the lowest activity, suggesting the presence of a previously undescribed autoinhibitory domain near the C-terminus. The inhibitory activity can be mapped to a small region at the extreme C-terminus of the kinase (residues 617−629) that exhibits sequence similarity to DMPK substrates. A peptide corresponding to these residues inhibits DMPK, indicating that this region likely functions as a pseudosubstrate inhibitor.

In an effort to define DMPK substrate specificity, we assessed the ability of recombinant DMPK to phosphorylate a panel of protein and peptide substrates. We observe that DMPK exhibits a novel catalytic activity similar to, but distinct from, known families of serine/threonine kinases. Endogenous activators of DMPK are unknown, but several members of the DMPK family are known to function as downstream effectors of the Rho family of small GTPases (*14*−*18*). We observe that DMPK purified from cells exposed to GTP-γ-S exhibits enhanced activity, an observation consistent with the hypothesis that DMPK, like other family members, may be regulated in vivo by G proteins.

EXPERIMENTAL PROCEDURES

Expression Constructs. An 1890 bp human DMPK cDNA (accession no. L08835) encoding the 629 residue full-length DMPK protein (accession no. NP_004400) was cloned into the mammalian expression vector pCINeo (Promega). The full-length DMPK cDNA was digested with *Xba*I to generate DMPKΔMA, a deletion of sequences encoding residues 550−629. The DMPKΔCC/MA construct, lacking sequences encoding residues 378−629, was derived from the full-length cDNA by PCR with an internal downstream primer (5′-CCGGTCATCACATGGCAGTGAGCCCGTC-3′). DMPKΔAI was created by deletion of nucleotides 1838−1890, resulting in truncation of C-terminal amino acids 614−629. Epitope-tagged constructs were prepared by appending a 9 residue hemagglutinin (HA) or 11 residue c-myc tag to the N-terminus of full-length DMPK. For expression in *Escherichia coli*, full-length DMPK and DMPKΔMA cDNAs were cloned in-frame into the *Eco*RI site of the prokaryotic expression vector pGEX-6P-1 (Pharmacia Biotech). To generate His-DMPK, the full-length cDNA was cloned into the pRSET expression vector (Invitrogen) to produce a recombinant protein with a 58 residue N-terminal polyhistidine purification tag. All constructs were sequenced to verify reading frame and correct sequence.

Subcellular Fractionation. Human left ventricular samples were obtained from normal donor hearts that could not be placed for transplantation. The tissue was ground under liquid nitrogen and Dounce homogenized at 4 °C with a motor-driven pestle in 10 volumes/g of tissue (wet weight) extraction buffer consisting of 20 mM Tris, pH 7.5, 100 mM NaCl, 20% (v/v) glycerol, and 1 mM DTT. Parallel extractions and fractionations were carried out with extraction buffer alone (−inhibitors) and with extraction buffer that was supplemented with our standard protease inhibitor cocktail of 2 mM EDTA, 1 mM AEBSF, 10 μg/mL aprotinin, and 0.1 mM leupeptin (+inhibitors). The homogenate was centrifuged at 1000*g* for 10 min at 4 °C to produce the low-speed pellet and the low-speed supernatant. The low-speed supernatant was centrifuged at 100000*g* for 1 h at 4 °C to generate the high-speed pellet and the high-speed supernatant. The pellet fractions were resuspended in extraction buffer and all fractions were aliquotted, quick-frozen in liquid nitrogen, and stored at −80 °C. For DMPK conversion experiments, fractions were incubated at 37 °C for 0−3 h, resolved by SDS−PAGE, and subjected to Western analysis.

The high-speed pellet was further subfractionated into separate salt-washed membrane and cytoskeletal fractions. To prepare salt-washed membranes, the high-speed pellet was incubated with extraction buffer containing 1.0 M NaCl on ice for 1 h. The salt-washed membranes were collected by centrifugation at 100000*g*, resuspended in extraction buffer, and stored at −80 °C. To prepare the cytoskeletal fraction, the high-speed pellet was incubated with extraction buffer containing 1% TX100 (SurfactAmpsX-100, Pierce) on ice for 1 h. The cytoskeletal fraction was collected by-

centrifugation at 100000*g*, resuspended in extraction buffer, and stored at −80 °C. The salt-wash supernatant and the TX100-soluble noncytoskeletal supernatant were also aliquotted, quick-frozen, and stored at −80 °C. In some experiments the resuspended salt-washed membranes were recentrifuged at 100000*g* to generate a membrane pellet (M_p) and a membrane-derived supernatant (M_s).

Protein Analysis. Protein concentrations were determined by a modified Lowry protein assay (*19*) with BSA as a standard. The proteins (10 μg/lane) were resolved on SDS−7.5% polyacrylamide gels and either stained with Coomassie or transferred to nitrocellulose Western blots. Ponceau S staining was used to verify transfer efficiency and visualize unstained standards, which were β-galactosidase, 116 kDa; fructose-6-phosphate kinase, 85 kDa; glutamate dehydrogenase, 56 kDa; and aldolase, 39 kDa (Boehringer). The membranes were blocked with 5% nonfat dry milk and probed with a 1:5000 dilution in TBST (50 mM Tris, pH 7.5, 150 mM NaCl, and 0.1% Tween 20) of a rabbit polyclonal antibody raised against recombinant DMPK (kind gift of Dr. Robert G. Korneluk) (*8*). This antibody recognizes authentic DMPK as confirmed by the results of Pham et al. (*9*). Polypeptides were visualized with a goat anti-rabbit secondary antibody conjugated to HRP followed by enhanced chemiluminescence (ECL) (Renaissance, NEN). Images of the Western blots were captured on an IS-1000 digital imaging system (Alpha Innotech Corp.) and analyzed by densitometry.

In Vitro Translation. Coupled in vitro transcription/translation reactions were carried out according to the manufacturer's instructions (TNT system, Promega). Reactions (100 μL) included 50 μL of reticulocyte lysate, 2 μg of DNA template, 8 μL of ^{35}S-methionine (10 mCi/mL), and 2 μL of T7 RNA polymerase; reactions were carried out at 30 °C for 2 h. For conversion experiments, translation reactions were first subjected to gel-filtration chromatography in order to purify full-length radiolabeled protein (as described below). An aliquot (5 μL) of the purified protein fraction was added to 25 μL of salt-washed membranes, and the reaction was incubated at 37 °C for 2 h.

Gel-Filtration Chromatography. Superdex 200 (Pharmacia) was used to prepare a 0.5 cm × 19 cm sizing column. The column was equilibrated with 50 mM Tris, pH 7.5, 150 mM NaCl, and 1 mM DTT and calibrated with the size standards ovalbumin (43 kDa) and aldolase (158 kDa). Each sample was prepared by passing a 100 μL in vitro translation reaction over a 2 mL Sephadex G-50 Fine column (Pharmacia) to remove excess free label. The desalted sample was adjusted to 100 μL in equilibration buffer and an 80 μL aliquot was applied to the column. Fractions (0.1 mL) were collected at a flow rate of 15 cm/h (3 mL/h). An aliquot (25 μL) of each fraction was subjected to scintillation counting to determine ^{35}S counts. Another aliquot (5 μL) of each fraction was assessed for total protein by Bradford assay.

Purification of GST-DMPKΔMA. Cultures of *E. coli* transformed with GST-DMPKΔMA were induced with 1 mM IPTG, grown at 30 °C for 4 h, and harvested by pelleting. Cell pellets were resuspended in 50 mM Tris, pH 8.0, 0.2 M NaCl, 5 mM DTT, 2 mM EDTA, 1 mM AEBSF, 0.1 mM leupeptin, and 10 μg/mL aprotinin and lysed by the addition of 1 mg/mL lysozyme for 20 min on ice, followed by the addition of 1% TX100 (Pierce, Surfact-Amps X-100) for 10 min on ice. All subsequent steps were performed at 4 °C. The lysate was centrifuged at 18000*g* for 30 min and the supernatant was incubated overnight with glutathione−Sepharose 4B beads (Pharmacia). The beads were washed 4 times with cold 50 mM Tris, pH 7.5, 150 mM NaCl, 5 mM DTT, and 2 mM EDTA. GST-DMPKΔMA was eluted from the beads by the addition of 50 mM Tris, pH 8.0, 10 mM glutathione, 5 mM DTT, 2 mM EDTA, 1 mM AEBSF, 0.1 mM leupeptin, and 10 μg/mL aprotinin, analyzed on Coomassie-stained SDS gels, and used directly in kinase assays.

Cell Culture and Transfections. Mammalian COS and BC_3-H1 cells were grown in Falcon 3083 flasks, in 15 mL of Dulbecco's modified Eagle's medium (DMEM) containing 20% fetal bovine serum, 10 mM HEPES, and 4 mM L-glutamine. Twenty-four hours prior to transfection, 100 mm plates were seeded to approximately 50% confluency. Cells were washed once with TBS (50 mM Tris, pH 7.5, and 150 mM NaCl) and then incubated for 2 h at 37° C with a transfection mixture including 30 μL of SuperFect transfection reagent (Qiagen) and 5 μg of plasmid DNA. Cells were washed once in TBS and then incubated 48 h in DMEM + 20% FBS.

Immunoprecipitation of Epitope-Tagged Constructs. Transfected cells were lysed in RIPA buffer (1× TBS, 1% TX100, 0.5% deoxycholic acid, and 0.1% SDS) supplemented with protease inhibitors (1 mM AEBSF, 10 μg/mL aprotinin, 0.1 mM leupeptin, and 2 mM EDTA). Lysates were centrifuged at 42000*g* for 1 h and supernatants were recovered and pooled. For each set of immunoprecipitations, supernatants were aliquotted prior to incubation with 1 μL/mL 9E10 antibody for 1 h at 4° C. Protein A−Sepharose beads (Pharmacia), 10μL/mL, were added and incubated for 1 h at 4° C with continuous mixing. Beads were washed twice in 1 mL RIPA, twice in 1 mL of RIPA + 1 M NaCl, and twice in TBS. For GTP-γ-S permeabilization experiments, transfected cells were washed twice with TBS and then incubated for 10 min at 37 °C in 1 mL of TBS + 0.02% β-escin + 100 μM GTP-γ-S. Following incubation, the permeabilization solution was aspirated, and cells were processed for immunoprecipitation as described above and used in kinase assays in triplicate. Equivalent amounts of enzyme within an experiment were verified by SDS−PAGE, followed by Coomassie staining and densitometry.

Kinase Assays: GST-DMPK Assays. Assays for kinase activity were performed in a volume of 40 μL with 25 mM Tris, pH 8.0, 5 mM glutathione, 2.5 mM DTT, 1 mM EDTA, 0.5 mM AEBSF, 0.05 mM leupeptin, 5 μg/mL aprotinin, 10 mM $MgCl_2$, 0.1 mM [γ-^{32}P]ATP (1.5 mCi/μmol) (NEN) and the indicated amount of enzyme and substrate for 1 h at 37 °C. Histone, myelin basic protein (MBP), or myosin light chain (all from Sigma) were present at 25 μg/mL (1 μg in 40 μL). Peptide substrates tested included Kemptide (LRRASLG, Sigma K-1127, Malantide (RTKRSGSVYEPLKI, Sigma A-3317), glycogen synthase residues 1−8 peptide analogue (PLSRTLSVAAKK, Sigma P-5307), epidermal growth factor receptor residues 650−658 peptide (VRKRTLRRL, Sigma V-2131), and neurogranin residues 28−43 peptide (AAKIQASFRGHMARKK, Promega V5611). Inhibitors tested included the naturally occurring protein kinase A inhibitor (PKI) residues 5−24 peptide, to be referred to as the PKI peptide (TTYADFIASGRTGRRNAIHD, Promega V5681), and myristoylated PKC-α residues 19−31

peptide, (myr-RFARKGALRQKNV, Promega 5691). Peptide substrates were present at 0.5 mM and peptide inhibitors were present at 10 μM final concentration. Purified rat brain PKC consisted primarily of the α and β isoforms (Promega V5261). The activator of PKA, cyclic adenosine monophosphate (cAMP) (Sigma), was used at a final concentration of 10 μM. Phosphatidylserine (PS) (Sigma) (500 μg/mL) 50 μg/mL diacylglycerol (DAG) (Sigma), and 0.5 mM $CaCl_2$ were used to activate PKC. Reactions were initiated with the addition of Mg/[γ-^{32}P]ATP and stopped with either Laemmli sample buffer or a modified Tris−Tricine gel sample buffer. Samples were heated to 100 °C for 5 min, cooled, and loaded onto either 7.5% or 15% acrylamide SDS gels or precast 10−20% acrylamide Tris−Tricine gels (BioRad) and electrophoresed for 3 h at 75 V. Resolution of peptide substrates on Tris−Tricine gels permits the unambiguous determination of peptide phosphorylation, as opposed to filter binding assays, in which spurious counts can be introduced from autophosphorylated kinases and contaminants. Gels were treated for 30 min with 10% glutaraldehyde (Fisher, reagent grade) to fix the peptides and proteins and extensively washed to remove [γ-^{32}P]ATP. Phosphorylated peptides and proteins were visualized with a Molecular Dynamics PhosphorImager and loading equivalency was verified by Coomassie staining. Coomassie-stained phosphopeptides and phosphoproteins were excised from the gels and quantitated by liquid scintillation counting. Specific phosphorylation activities were calculated after subtraction of the background counts found in the substrates incubated in the absence of GST-DMPKΔMA from the total counts found in the presence of GST-DMPKΔMA.

(B) Immunoprecipitation Kinase Assays. Kinase assays were performed on immunoprecipitated DMPK including 10 μL of washed beads, 20 mM Tris, pH 7.5, 10 mM $MgCl_2$, and 0.1 mM [γ-^{32}P]ATP (1.5 mCi/μmol) (NEN) in a total volume of 40 μL. EGFR peptide substrate (VRKRTLRRL, Sigma V-2131) was present in concentrations ranging from 0 to 1 mM. Reactions were initiated with the addition of Mg/[γ-^{32}P]ATP and stopped with a modified Tris−Tricine gel sample buffer. Although DMPK activity was observed to remain linear up to an hour, immunoprecipitation kinase assays were carried out for 15 min at 37 °C. Kinase reactions were resolved on Tris−Tricine 16.5% polyacrylamide gels alongside a range of known concentrations of BSA standard, fixed and stained as described above. Stained gels were imaged (IS-1000 digital imaging system, Alpha Innotech Corp.); densitometry measurements of the BSA standards and DMPK bands allowed generation of a protein standard curve, quantitation of immunoprecipitated DMPK in each kinase reaction (typically about 1 μg of recombinant kinase), and verification of recovery equivalency. Coomassie-stained phosphopeptides were excised from the gels and quantitated by scintillation counting. V_{max} values were calculated by using the Solver function of Microsoft Excel to generate a least-squares fit of the v/[A] curve of the kinetic data to the Michaelis equation. C-Terminal peptide inhibition studies were carried out with immunoprecipitated DMPKΔAI, a fixed concentration of EGFR peptide substrate (500 μM, the calculated K_m for this substrate), and a range of concentrations of C-terminal peptide. Activity data were analyzed with a Dixon plot (1/V vs [I]). Apparent K_i was determined by solving the shown linear equation where $x = -K_i$ and $y = 1/V_{max}$.

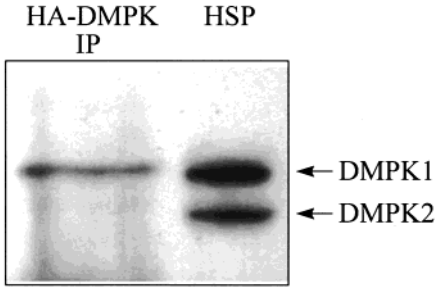

FIGURE 2: Endogenous DMPK-1 corresponds to the full-length translation product. A full-length DMPK cDNA construct was engineered with a small 9 amino acid hemagglutinin (HA) epitope tag. In vitro expressed DMPK was immunoprecipitated (IP) and compared to a left ventricular high-speed pellet fraction (HSP) by Western blot. Full-length DMPK (predicted 70 kDa) migrates anomalously at approximately 89 kDa and corresponds to endogenous DMPK-1.

RESULTS

Origin of DMPK forms: (A) Origin of DMPK-1. The predicted molecular mass of full-length DMPK (69 kDa) is closer to the apparent molecular mass of endogenous DMPK-2 (~80 kDa). However, since proteins often run anomalously in SDS−PAGE we compared endogenous DMPK to in vitro expressed full-length DMPK of known size. Full-length DMPK with a small 9 amino acid HA epitope tag (predicted molecular mass 70 kDa) was expressed in vitro, isolated by immunoprecipitation, and resolved by SDS−PAGE adjacent to a human heart fraction. Western analysis with an anti-DMPK antibody (Figure 2) demonstrated that HA-DMPK migrated anomalously large as a single band with an apparent molecular mass of 89 kDa, just slightly larger than endogenous DMPK-1. Commercial reticulocyte lysate may support some degree of posttranslational modification of recombinant proteins and thus it is possible that a smaller product has been modified into a larger product. However, we observed a single recombinant protein product and it is unlikely that such modification would be complete and quantitative in the absence of supplemental microsomes. These results are in agreement with observations by Maeda et al. (*7*) who found no evidence of posttranslational modification of endogenous DMPK, and are consistent with the initial full-length translation product of the DMPK gene being DMPK-1.

(B) Conversion of Endogenous DMPK-1 to DMPK-2. If DMPK-1 is the initial translation product, it should be possible to observe the conversion of DMPK-1 into DMPK-2 in tissue extracts. This converting activity is likely to be a protease since DMPK-2 is smaller than DMPK-1. To test this supposition, human heart tissue was subfractionated (described under Experimental Procedures) in the presence and absence of our standard protease inhibitor cocktail. The fractions were incubated at 37° C for 2 h and subjected to Western analysis with the anti-DMPK antibody. With incubation the amount of DMPK-1 decreased and the amount of DMPK-2 increased, suggesting that DMPK-1 was converted into DMPK-2. This is unlikely to be nonspecific degradation because the sum total amount of DMPK forms did not decrease. The conversion was partially blocked by

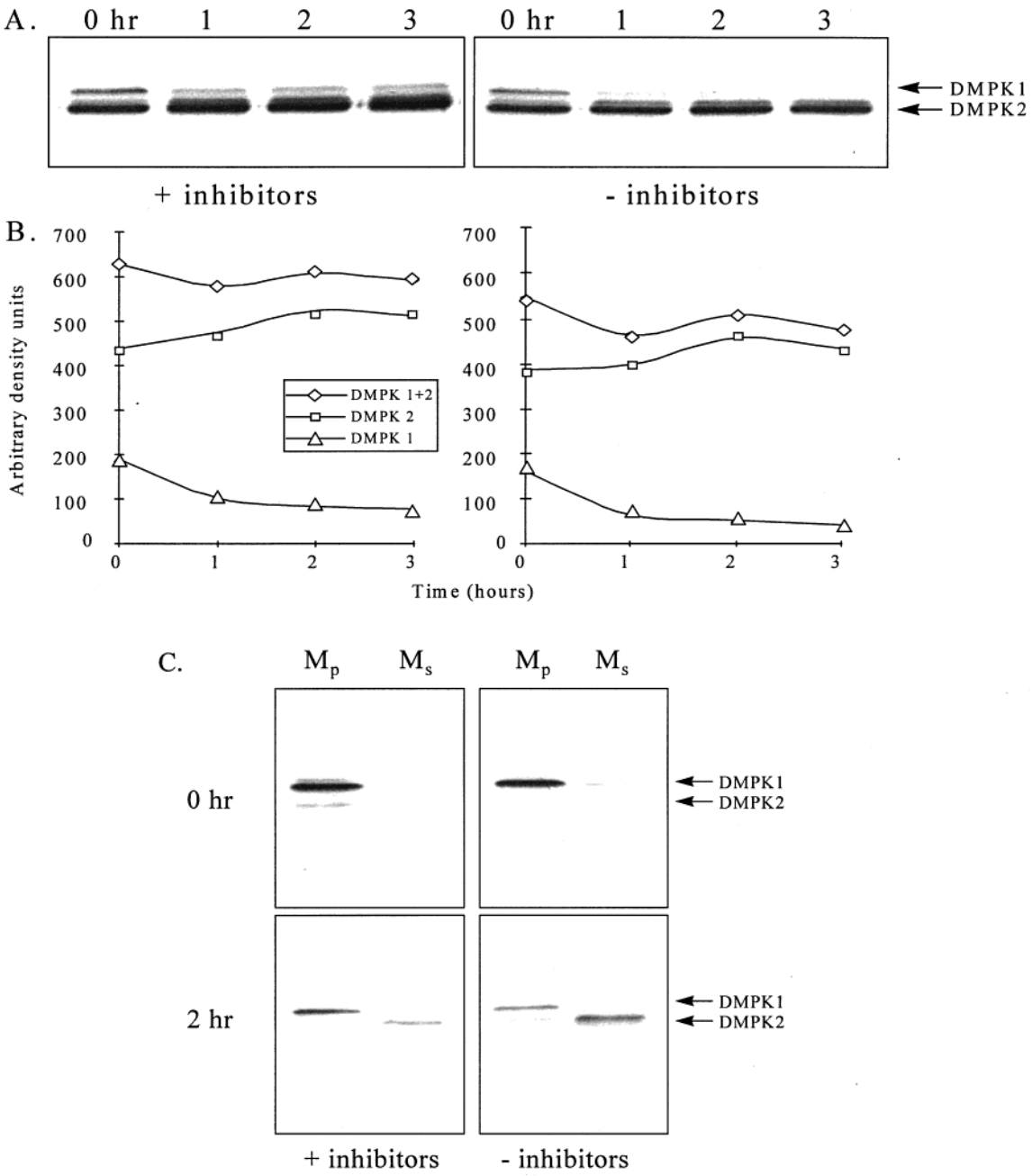

FIGURE 3: Conversion of endogenous DMPK-1 into DMPK-2. (A) High-speed pellet fractions prepared in the presence or absence of protease inhibitors were incubated at 37° C for 0, 1, 2, and 3 h. The time-dependent decrease in DMPK-1 was associated with a corresponding increase in DMPK-2, indicating that DMPK-1 is converted into DMPK-2. The conversion was partially blocked by the protease inhibitor cocktail. (B) Relative amounts of DMPK-1, DMPK-2, and DMPK-1 + DMPK-2 were determined by densitometry and plotted as a function of time of incubation. (C) Membrane conversion of DMPK-1 and release of DMPK-2 into the supernatant. Resuspended salt-washed membranes prepared in the presence or absence of protease inhibitors (top panels) were incubated at 37° C for 2 h (bottom panels) and then centrifuged at 100 000*g* to reisolate the membranes (M_p) and generate a membrane-derived supernatant (M_s). DMPK-1 remained associated with the membrane pellet, but soluble DMPK-2 generated from DMPK-1 conversion was released into the supernatant.

the protease inhibitor cocktail. By observing the extent of conversion in the various fractions we could follow the converting activity (data not shown). This activity was observed in the homogenate fraction, and after low-speed centrifugation, the activity was found in the low-speed supernatant. The low-speed supernatant was subjected to high-speed centrifugation, and the converting activity segregated to the high-speed pellet. A time course of conversion was performed (Figure 3A) on the high-speed pellet. As concentrations of DMPK-1 decreased there was a corresponding increase in concentrations of DMPK-2, while the total of DMPK-1 and DMPK-2 remained relatively constant as determined by densitometry of Western blots (Figure 3B). These data suggest that DMPK-1 and DMPK-2 are in a precursor/product relationship, with DMPK-1 being converted into DMPK-2.

The high-speed pellet consists primarily of membrane and cytoskeletal components, so it was further subfractionated as described under Experimental Procedures to determine the localization of the converting activity (data not shown). The cytoskeletal fraction consisted predominantly of actin and myosin, as determined from gel staining, and a portion of DMPK-1 and DMPK-2 was associated with the cytoskeletal fraction, as determined by Western blotting. Con-

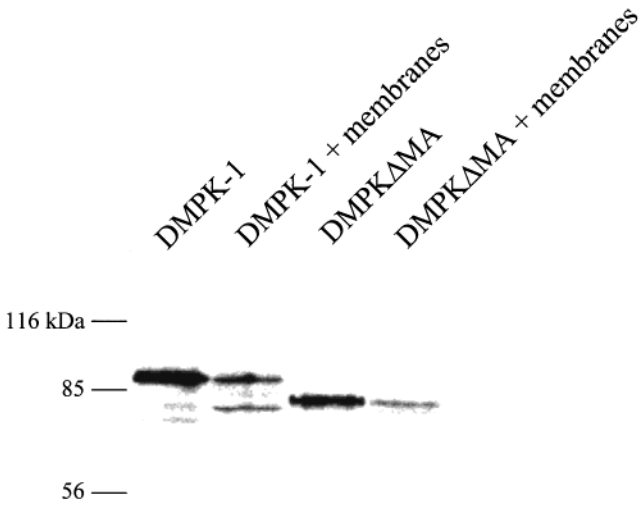

FIGURE 4: Conversion of recombinant in vitro translated DMPK-1 into DMPK-2 by human heart membranes. Full-length radiolabeled DMPK-1 and DMPKΔMA were generated by in vitro translation in the presence of ^{35}S-methionine and purified by gel filtration. Purified proteins were incubated with and without a fraction of salt-washed membranes from human heart. The products were resolved by SDS−polyacrylamide gel electrophoresis and visualized by PhosphorImager analysis. The proteolytic processing activity of the membranes converted the recombinant DMPK-1 to DMPK-2.

versely, actin and myosin were the major proteins released by salt wash of the membranes, demonstrating the selectivity of the subfractionation. The subfractions were incubated and analyzed by Western blotting. The conversion was observed in the membrane fraction and to a lesser extent in the noncytoskeletal fraction, which consists mainly of TX100-solubilized membrane proteins. These results suggest that the converting activity resides in a membrane-associated protease. As before, the protease inhibitors partially inhibited the conversion. The conversion experiment was repeated but the resuspended salt washed membranes were centrifuged to reisolate the membranes (M_p) and generate a membrane-derived supernatant (M_s). The resulting samples were analyzed by SDS−PAGE and Western blotting (Figure 3C). DMPK-1 remained associated with the membrane pellet, while the DMPK-2 that was produced was soluble and found in the supernatant fraction.

(C) Conversion of Recombinant DMPK-1 to DMPK-2. To confirm these observations by an independent method, we repeated the processing experiments using labeled recombinant DMPK. This technique offers the advantage that all proteolytic products can be detected, since DMPK is uniformly labeled. We expressed full-length DMPK-1 and DMPKΔMA (a truncated kinase lacking the C-terminal membrane association domain) in vitro, using ^{35}S-methionine to label the proteins. Full-length recombinant protein was purified away from incomplete translation products by gel filtration chromatography (see Experimental Procedures). Addition of a salt-washed human heart membrane fraction to recombinant DMPK-1 caused conversion of full-length kinase into DMPK-2, but DMPKΔMA was not similarly converted (Figure 4). Since DMPK-1 and DMPKΔMA share the same N-terminus, these observations indicate that cleavage occurs at the C-terminus of the kinase. If proteolysis had occurred at the N-terminus, DMPKΔMA would also have exhibited a similar (approximately 8 kDa) decrease in size.

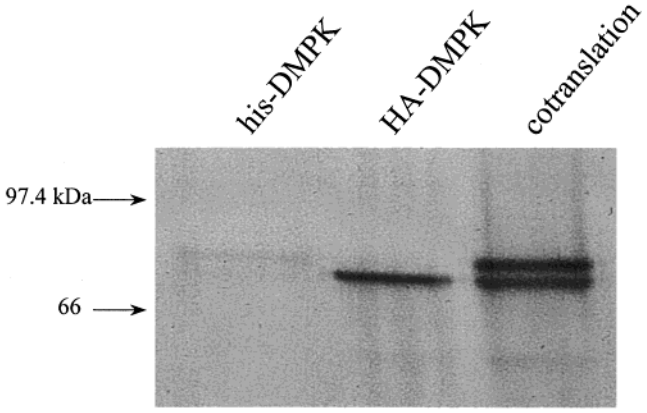

FIGURE 5: In vitro translated DMPK self-associates. HA-tagged DMPK (apparent molecular mass 88 kDa) and His-tagged DMPK (apparent molecular mass 91 kDa) were either expressed separately or coexpressed in vitro in the presence of ^{35}S-methionine. Translation mixtures were immunoprecipitated with an anti-HA antibody, resolved by SDS−PAGE, and visualized by autoradiography. His-DMPK is not precipitated by the HA antibody but coprecipitates when coexpressed with HA-DMPK.

DMPK Oligomerization and Activity: (A) DMPK Self-Association. Previous observations have suggested that recombinant and native DMPK is multimeric (*9, 20*). Consistent with this notion, we observed that in vitro expressed DMPK was able to self-associate (Figure 5). When expressed alone, larger His-DMPK without the HA epitope tag did not immunoprecipitate with an anti-HA antibody. However, when His-DMPK was coexpressed with the smaller HA-DMPK construct, the HA antibody immunoprecipitated both forms, indicating that His-DMPK is able to interact with HA-DMPK. To more precisely map the domains required for oligomerization, we performed gel-filtration sizing chromatography of in vitro expressed domain-deleted DMPK forms.

DMPK C-terminal domain-deleted constructs utilized in gel-filtration chromatography and subsequent immunoprecipitation kinase assays are shown in Figure 1. All constructs possess an 11 residue c-myc epitope tag appended in frame with the N-terminus. The full-length construct possesses all native domains and encodes a protein with a predicted molecular mass of 70.6 kDa (with an apparent molecular mass in SDS−PAGE approximately 88 kDa). DMPKΔMA lacks the C-terminal membrane association domain and encodes a protein of predicted 63.5 kDa (with an apparent molecular mass in SDS−PAGE approximately 80 kDa), and closely corresponds in size to endogenous DMPK-2. DMPKΔCC/MA lacks sequences C-terminal to the catalytic domain, including both coiled-coil and membrane association domains, and encodes a protein of 44 kDa.

(B) Gel-Filtration Sizing Chromatography. We chose to examine the oligomerization properties of DMPK by nondenaturing gel-filtration chromatography, a method that has proven useful in the study of other coiled-coil proteins (*21*). Full-length DMPK, DMPKΔMA, and DMPKΔCC/MA were expressed in vitro as ^{35}S-methionine labeled proteins. Reaction mixtures were passed over a Sephadex G-50 Fine column to remove excess free label, and then applied to a Superdex 200 gel-filtration sizing column (preparation and

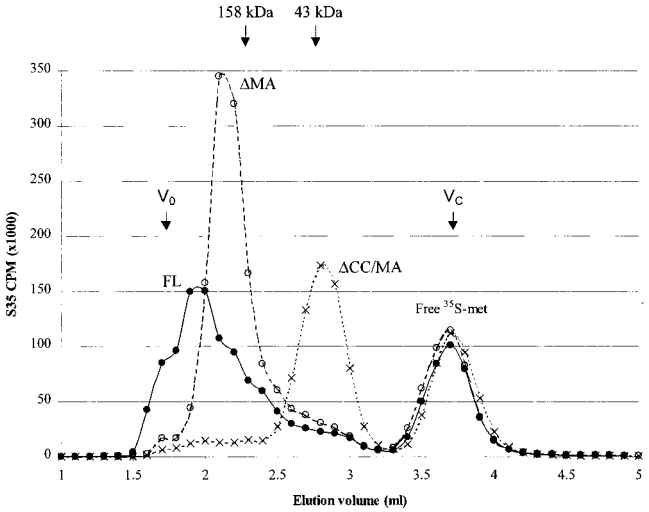

FIGURE 6: Coiled-coil and membrane association domains strongly influence sizes of DMPK forms. DMPK domain-deletion forms were expressed in vitro and separated by Superdex 200 gel-filtration chromatography. The elution profiles of DMPKΔCC/MA (×), DMPKΔMA (○) and full-length DMPK (●) were generated by measuring ^{35}S counts in each fraction. Positions of size standards aldolase (158 kDa) and ovalbumin (43 kDa) are indicated.

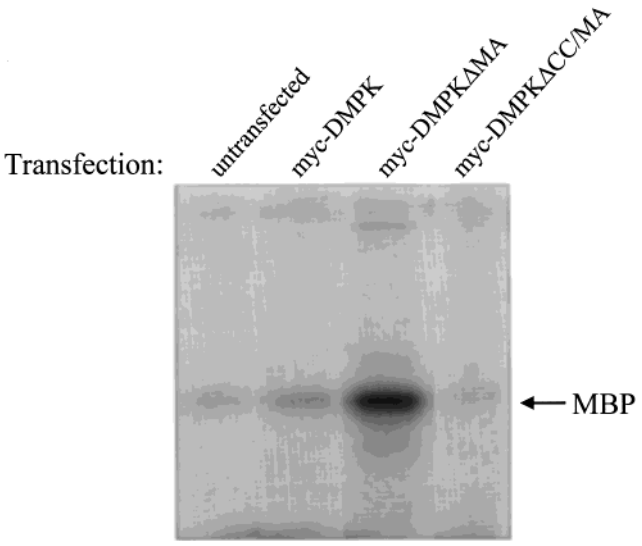

FIGURE 7: Catalytic activity of DMPK forms correlates with ability to oligomerize. Immunoprecipitation kinase assays were performed on myc epitope-tagged DMPK forms expressed in mammalian cells and immunoprecipitated with anti-myc antibody. Kinase reactions utilized myelin basic protein (MBP) as an in vitro substrate and were visualized by PhosphorImager analysis. Specific activities were calculated by normalizing kinase activity to DMPK protein as measured by densitometry of parallel Western blots. With the activity of full-length DMPK arbitrarily set to 1, the normalized specific activities were 5.8 for DMPKΔMA, and 2.0 for DMPKΔCC/MA.

calibration described under Experimental Procedures). Column fractions were analyzed by scintillation counting to monitor the elution profiles of labeled protein species. The combined elution profiles of the three proteins are shown in Figure 6; SDS−PAGE and autoradiography of peak fractions confirmed that ^{35}S peaks resolved by gel filtration corresponded to the anticipated DMPK forms (not shown). DMPKΔCC/MA protein eluted from the sizing column in a single peak of the expected size of a monomer, approximately 50 kDa. In contrast, DMPKΔMA protein containing the coiled-coil domain was recovered in a single peak corresponding to approximately 250 kDa, much larger than the expected 63.5 kDa for a DMPKΔMA monomer. This observation suggests that the coiled-coil domain mediates the formation of a single oligomeric species. However, a portion of DMPKΔMA may remain monomeric, indicated by the presence of a small shoulder to the right of the main peak. Full-length DMPK protein containing both coiled-coil and membrane association domains eluted with a much higher apparent molecular mass, approximately 900 kDa. The elution profile of full-length DMPK exhibits several "shoulders", indicating the presence of a number of discrete complexes of various sizes. This suggests that the hydrophobic membrane association domain causes association of DMPK oligomers into larger aggregates composed of multiple DMPK oligomers.

(C) Immunoprecipitation Kinase Assays. To assess the effects of the loss of the coiled-coil and membrane association domains upon catalytic activity, we expressed full-length DMPK, DMPKΔMA, and DMPKΔCC/MA in mammalian cells and performed immunoprecipitation kinase assays with myelin basic protein (MBP) as a substrate (Figure 7). DMPKΔMA exhibited robust catalytic activity, while full-length DMPK and DMPKΔCC/MA activities were near background levels. Specific activities for the three constructs were calculated by normalizing kinase activity to DMPK protein levels as measured by densitometry of parallel Western blots. Interestingly, full-length DMPK appeared to be relatively catalytically inactive, exhibiting approximately 6-fold lower activity than DMPKΔMA. Compared to oligomeric DMPKΔMA, oligomerization-defective DMPKΔCC/MA exhibited an approximately 3-fold lower kinase activity. DMPKΔCC/MA did retain some catalytic activity, however, with approximately twice the activity of full-length kinase.

DMPK Substrate and Inhibitor Specificity. As an alternative approach for the production and characterization of recombinant DMPK, we expressed full-length DMPK in *E. coli* as a GST fusion protein. Full-length DMPK was poorly expressed in a variety of strains (not shown), possibly due to toxicity caused by the hydrophobic C-terminal membrane association domain. A C-terminally truncated construct, GST-DMPKΔMA (a deletion of amino acids 550−629, including the membrane association domain but not the coiled-coil), could be expressed and purified from TOP10F′ cells.

Purified GST-DMPKΔMA was enzymatically active, exhibiting autophosphorylation and phosphorylation of the general kinase substrates histone and myelin basic protein; interestingly, myosin light chain, a known substrate of the closely related Rho kinase subfamily, was not phosphorylated by GST-DMPKΔMA (not shown). On the basis of catalytic domain sequence homology, DMPK has frequently been described as being related to protein kinases PKA and PKC. In an effort to compare the activity of DMPK to these well-characterized kinases, we challenged GST-DMPKΔMA with known PKA and PKC peptide substrates and inhibitors. PKA substrates included the classic Kemptide (LRRASLG) (*22*) and Malantide (RTKRSGSVYEPLKI) (*23*). PKC substrates were the glycogen synthase (GS) residues 1−8 peptide analogue (PLSRTLSVAAKK) and the epidermal growth factor receptor (EGFR) residues 650−658 peptide (VRKRTLRRL) (*24*). GST-DMPKΔMA did not phosphorylate either Kemptide (Figure 8A) or Malantide (not shown) but did

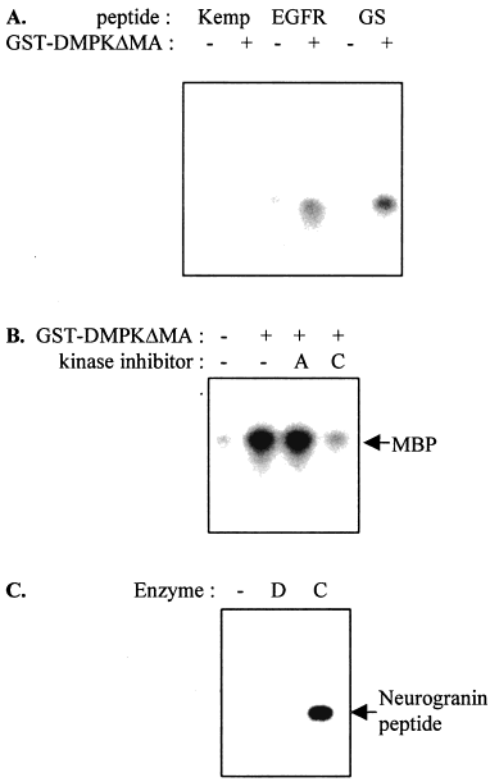

FIGURE 8: DMPKΔMA phosphorylates some PKC peptide substrates and is inhibited by the myr-ψPKC peptide but does not phosphorylate a PKC-specific neurogranin peptide. (A) Kinase assays were performed with 50 ng of GST-DMPKΔMA and either Kemptide, EGFR peptide, or GS peptide. (B) Kinase assays were performed with 50 ng of GST-DMPKΔMA, 1 μg of MBP, and either 10 μM PKI peptide (lane A) or 10 μM myr-ψPKC peptide (lane C). (C) Kinase assays were performed with 50 ng of GST-DMPKΔMA (lane D) or 50 ng of PKC (lane C) and a peptide modeled on neurogranin residues 28−40. This peptide, the most specific peptide substrate for PKC, was not a substrate for GST-DMPKΔMA. All reactions were stopped with a modified sample buffer and the samples were resolved on 10−20% acrylamide Tris−Tricine gels and fixed with glutaraldehyde. Phosphorylation was visualized by PhosphorImager and loading equivalency was verified by Coomassie staining (not shown).

phosphorylate both the GS peptide and the EGFR peptide (Figure 8A). Although the GS peptide can be phosphorylated by other kinases (*25*), it has been used to specifically assay PKC activity in permeabilized T lymphocytes (*26*). The EGFR peptide was not known until now to be phosphorylated by any kinase other than PKC (*25*). These results indicate that DMPK, which is more closely related by sequence to PKA, actually has a phosphorylation site motif preference more similar to that of PKC.

Sensitivity of a kinase to specific peptide inhibitors can provide information regarding substrate specificity, since peptide inhibitors derived from autoinhibitory pseudosubstrate regions often display higher affinities and specificities to their corresponding kinases than peptide substrates (*27*). To further refine the substrate specificity of DMPK, we examined the sensitivity of GST-DMPKΔMA to specific peptide inhibitors of PKA and PKC. The PKI peptide (TTYADFIASGRTGRRNAIHD) corresponds to residues 5−24 of the naturally occurring PKA inhibitor PKI (*28*). The myr-ψPKC peptide (myr-RFARKGALRQKNV) corresponds to residues 19−31 of PKC-α, the autoinhibitory pseudosubstrate domain (*29*, *30*). As shown in Figure 8B,

Table 1: DMPK Peptide Substrates and Inhibitors

MBP residues 106-113 peptide:				G	**R**	G	L	**S**	**L**	S	**R**			
GS peptide:	P	L	S	**R**	T	L	**S**	**V**	A	A	K	K		
EGFR peptide:				V	**R**	K	R	**T**	**L**	**R**	R	L		
myr-ψPKC inhibitor:				F	A	**R**	K	*G*	*A*	**L**	**R**	Q	K	N	V
DMPK C-term. aa 617-629:	T	A	V	W	R	**R**	P	*G*	*A*	A	**R**	A	P		
DMPK consensus motif:						**R**	**x**	**x**	**S/T**	**L/V**	**R**				

the phosphorylation of MBP by GST-DMPKΔMA was not inhibited by 10 μM PKI peptide but was 82% inhibited by 10 μM myr-ψPKC peptide. The PKI peptide is very specific and at this concentration would maximally inhibit PKA but not affect any other kinases (*31*). The myr-ψPKC peptide is not quite as specific but had an IC_{50} of 7−8 μM against TPA-activated PKC in fibroblasts (*30*). Since we observed an 82% inhibition with 10 μM, the IC_{50} for this inhibitor against GST-DMPKΔMA must be lower than 10 μM and close to that for PKC itself. The IC_{50}s of this inhibitor for calcium/calmodulin dependent protein kinase II (CaMK-II) and MLCK are 30 μM and 35 μM, respectively (*31*), and these enzymes would only be slightly inhibited at the concentration used. In terms of its sensitivity to peptide inhibitors, GST-DMPKΔMA was distinct from PKA, CaMK−II, and MLCK but more similar to PKC.

We compared the substrate specificities of DMPK and PKC in greater detail by examining the ability of GST-DMPKΔMA to phosphorylate a neurogranin residues 28−43 peptide (AAKIQASFRGHMARKK). This peptide is the most potent and specific peptide substrate known for PKC (*32*) and is often used to assay PKC activity in crude extracts containing other kinases. As shown in Figure 8C, the neurogranin peptide was highly phosphorylated by PKC but was not a substrate for DMPK. Thus, while the substrate specificity of DMPK exhibits substantial overlap with that of PKC, it is clearly distinct.

The only peptide previously shown to be a DMPK substrate, MBP residues 106−113 peptide (*33*), is also a substrate for PKA and PKC (*34*). The phosphorylation of the GS and EGFR peptides by GST-DMPKΔMA and the potent inhibition of the kinase by the myr-ψPKC peptide allowed us to derive a putative DMPK consensus phosphorylation motif (see Table 1).

Enzyme Kinetics and Autoinhibition. To facilitate a more detailed kinetic analysis of DMPK activity, we decided to express myc epitope-tagged recombinant DMPK in mammalian cells. This approach had several advantages over prokaryotic expression: transiently transfected mammalian cells produced greater quantities of recombinant protein, purification was simplified by immunoprecipitation, and full-length DMPK could be expressed. Velocity curves (Figure 9) were generated for DMPK forms; EGFR peptide was used as a substrate because it has a single phosphorylation site whereas protein substrates such as MBP have multiple potential phosphorylation sites, complicating kinetic analysis. A least-squares fit of the v/[A] curve of the Michaelis equation was used to derive the V_{max} for each DMPK form. Under these conditions, DMPKΔMA exhibited a basal catalytic activity (V_{max}) of 410 pmol min^{-1} mg^{-1}. As previously observed, full-length DMPK was relatively inactive, reaching saturation at low substrate concentrations and exhibiting a V_{max} of 160 pmol min^{-1} mg^{-1}. Enzyme was

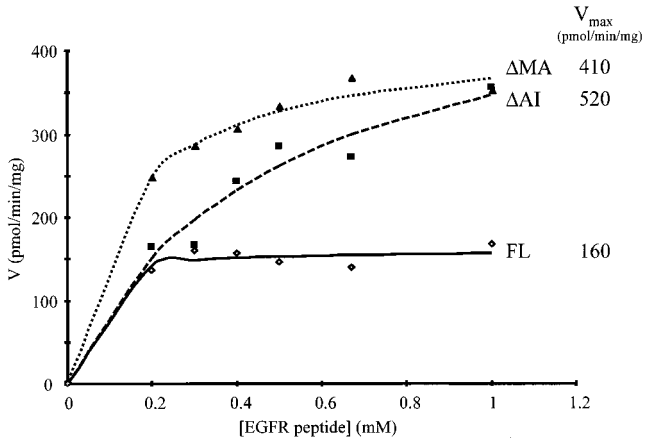

FIGURE 9: Enzyme kinetics of DMPK forms. Myc epitope-tagged DMPK forms were expressed in mammalian cells, immunoprecipitated, and used in kinase assays with a range of substrate concentrations (EGFR peptide substrate). Phosphorylated peptide was resolved on Tris−Tricine gels, fixed, stained, and excised for counting. Curves represent a least-squares fit of the data to the Michaelis equation. Full-length DMPK reaches saturation and exhibits low activity relative to the ΔMA and ΔAI forms. DMPKΔAI (lacking the 16 amino acid putative autoinhibitory domain) exhibits a greater than 3-fold increase in V_{max} relative to the full-length kinase. A similar increase in activity is observed for DMPKΔMA, which closely corresponds to the in vivo processed form of the kinase, DMPK-2.

quantitated by densitometry of Coomassie stained gels, possibly leading to some degree of imprecision in these values; however, the relative activities of the DMPK forms were found to be highly reproducible.

This unexpected observation suggested the presence of an autoinhibitory domain in the C-terminal portion of DMPK. The substrate and inhibitor studies had allowed us to derive a tentative DMPK phosphorylation motif, **R x x S/T L/V R** (Table 1). An examination of C-terminal DMPK sequences revealed a candidate pseudosubstrate autoinhibitory sequence in amino acids 617−629 (TAVWRRPGAARAP). This sequence is similar to that of the myr-ψPKC peptide and contains the **R x G A** motif that is absolutely conserved in all PKC pseudosubstrate domains from yeast to man (*27*). To assess the effects of loss of this sequence upon catalytic activity we generated DMPKΔAI, a truncation construct lacking the 16 C-terminal amino acids 614−629. Kinetic analysis (Figure 9) confirmed that DMPKΔAI exhibited a greater than 3-fold increase in V_{max} (520 pmol min^{-1} mg^{-1}) relative to full-length kinase.

To test whether the putative autoinhibitory sequence could inhibit DMPK activity in trans, we had the peptide sequence synthesized (TAVWRRPGAARAP) and carried out standard DMPK kinase assays with a range of concentrations of the C-terminal peptide. When the EGFR substrate was presented at its K_m (500 μM), this synthetic peptide inhibited DMPKΔAI activity with an apparent K_i of 7.5 μM (Figure 10), providing further evidence that this sequence functions as an in vivo autoinhibitory motif.

DMPK Activation. Many protein kinases are regulated by interactions with regulatory molecules that act to transiently stimulate kinase activity. Since physiological activators of DMPK are unknown, the kinase activity we observe with recombinant DMPK likely represents basal catalytic activity. In an effort to determine whether activators of known kinases

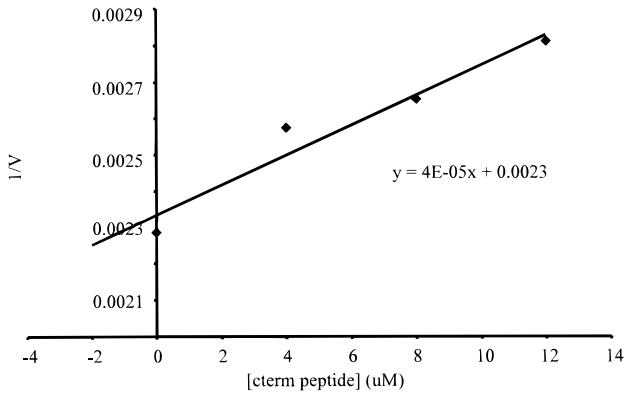

FIGURE 10: Synthetic peptide corresponding to DMPK residues 617−629 inhibits DMPKΔAI kinase activity. DMPKΔAI immunoprecipitation kinase assays were carried out with an EGFR peptide substrate (500 μM) and a range of concentrations of the C-terminal peptide. Inhibition data are presented as a Dixon plot ($1/V$ vs [I]). The calculated K_{iapp} for the C-terminal peptide is 7.5 μM.

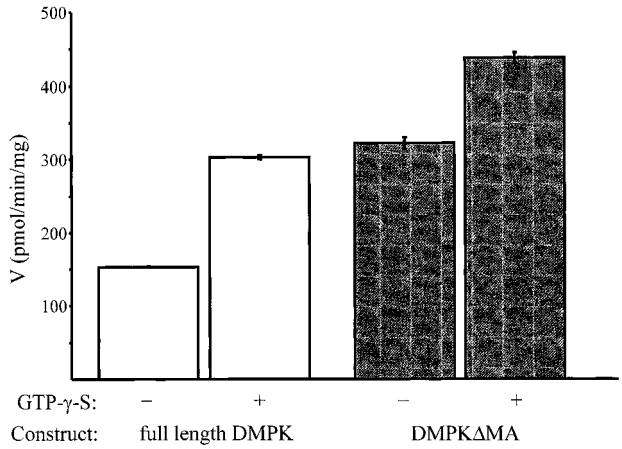

FIGURE 11: DMPK purified from cells exposed to GTP-γ-S exhibits enhanced catalytic activity. Transiently transfected mammalian cells expressing myc epitope-tagged DMPK were permeabilized with 0.02% β-escin in the presence or absence of 100 μM GTP-γ-S. DMPK was immunoprecipitated from permeabilized cells and kinase assays were performed with the EGFR peptide substrate (500 μM). The activity (average ± SE) of full-length DMPK increased 2-fold with GTP-γ-S treatment ($p < 0.0001$). DMPKΔMA has a higher basal activity due to the absence of the autoinhibitory domain but also exhibits increased activity with exposure to GTP-γ-S ($p = 0.0004$).

also stimulate DMPK, we examined the effects of PKA and PKC activators upon DMPK activity (not shown). GST-DMPKΔMA activity was not affected by addition of either 10 μM cAMP (PKA activator) or 500 μg/mL PS, 50 μg/mL DAG, and 0.5 mM $CaCl_2$ (PKC activators). The basal activity of GST-DMPKΔMA appeared to be comparable to the basal activity of unstimulated PKC.

Small G proteins represent another class of potential DMPK activators, since several members of the DMPK family are regulated by Rho family GTPases. To examine this possibility, we immunoprecipitated DMPK from transfected mammalian cells that had been permeabilized with 0.02% β-escin and exposed to 100 μM GTP-γ-S, a potent activator of endogenous G proteins. GTP-γ-S treatment increased full-length DMPK activity 2-fold (Figure 11). This stimulation of activity was in addition to that conferred by removal of the autoinhibitory domain, as DMPKΔMA

activity was also increased by GTP-γ-S. While a 2-fold increase in activity is modest, the stimulation was significant ($p < 0.0001$) and represents a similar degree of stimulation to that reported for Rho kinase activated by Rho-GTP (*14*). These results are consistent with the ability of DMPK to be regulated by G proteins but do not demonstrate activation by direct binding of a specific small GTPase. We examined the effects of Rho-GTP, Rac-GTP, and Cdc42-GTP upon DMPK activity, but found no evidence that DMPK is activated by any of these small GTPases (not shown).

DISCUSSION

Our studies demonstrate that full-length recombinant DMPK is equivalent in size to endogenous DMPK-1, indicating that DMPK-1 represents the primary translation product. We observe conversion of DMPK-1 to DMPK-2 in a time-dependent, protease inhibitor-sensitive process, demonstrating that the conversion event is likely caused by proteolysis of DMPK-1. The processing activity can be fractionated to a salt-washed membrane fraction consistent with a membrane-bound protease. Previous observations in our laboratory indicated that DMPK-1 is more tightly associated with membranes than DMPK-2 (*7*). The current study confirms and extends these observations, demonstrating that proteolytic processing converts endogenous membrane-associated DMPK-1 to soluble DMPK-2. In addition, recombinant full-length DMPK-1 can be converted to DMPK-2, but a DMPK form lacking C-terminal sequences (DMPKΔMA) is not similarly converted. The most reasonable explanation for these observations is that the proteolytic cleavage that generates DMPK-2 removes the C-terminal hydrophobic membrane association domain. Consistent with this hypothesis, observations of recombinant DMPK expressed in insect cells confirm that full-length DMPK remains membrane-associated, whereas DMPK lacking the membrane association domain is cytosolic (*10*).

We have further demonstrated that the DMPK coiled-coil domain is required for oligomerization of the kinase. DMPK oligomerization also correlates with activity, strongly suggesting that coiled-coil mediated oligomerization is important for enhanced basal catalytic activity. Whether the DMPK oligomer is a dimer or higher order multimer remains to be determined. While coiled-coil domains typically mediate the formation of protein dimers, they can also form trimers and tetramers (*12, 21, 35, 36*). DMPKΔMA eluted from the sizing column at a volume corresponding to a globular protein of approximately 250 kDa. This observation is consistent with either a globular DMPKΔMA tetramer or an asymmetric DMPKΔMA dimer/trimer that migrates anomalously in gel-filtration due to secondary structure such as the rod-shaped coiled-coil domain. The 77 amino acids that form the DMPK coiled-coil display the characteristic periodic distribution of hydrophobic residues within a series of 11 heptad repeats [determined by the COILS algorithm (*37*)]. The abundance of leucine residues in the *d* heptad position and charged residues in the *e* and *g* positions indicate that the DMPK coiled-coil is likely to form dimers (*21, 36*).

Our studies of protein substrates, peptide substrates, and peptide inhibitors indicate that DMPK exhibits an in vitro phosphorylation motif preference that is somewhat similar to PKC. DMPK apparently favors an arginine upstream of the phosphoacceptor site (serine or threonine), followed by a hydrophobic residue (leucine or valine), followed by another arginine. This in vitro consensus motif, **R x x S/T L/V R**, is similar to that of PKC in preferring upstream and downstream basic residues and is similar to that of CamK II and phosphorylase kinase in preferring a downstream hydrophobic residue (*25*). Thus, the DMPK phosphorylation motif appears to be overlapping yet distinct from previously described classes of kinases.

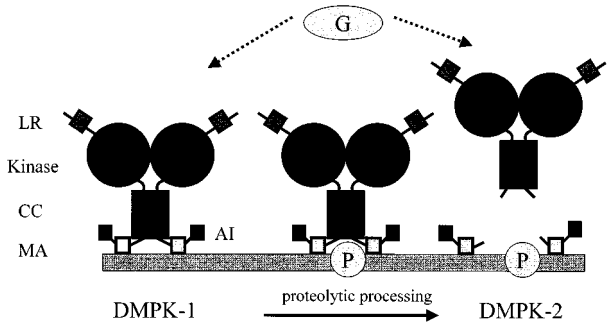

FIGURE 12: Model for DMPK oligomerization, processing and regulation. Full-length DMPK monomers oligomerize via coiled-coil domains to produce membrane-associated DMPK-1. DMPK-1 oligomers exhibit low basal catalytic activity due to the presence of the C-terminal autoinhibitory domain (AI). A protease (P) within the membrane cleaves DMPK-1, removing the C-terminal autoinhibitory and membrane association domains and releasing cytosolic, basally active DMPK-2. This processing event would produce long-term activation of the kinase. Short-term activation of DMPK-1 and -2 may be mediated by transitory interaction with a small GTPase (G).

Sequence comparisons suggest that the DMPK family of kinases is further divided into subfamilies. These subfamilies are likely to be distinguished by unique substrate specificities. The Rho kinases have been shown to phosphorylate myosin light chain at an SNVF motif, the same site utilized by myosin light-chain kinase (*38*). Our results indicate that myosin light chain is not phosphorylated by DMPK, suggesting that DMPK catalytic activity is distinct from that of the Rho kinases. Human PK428, however, is more closely related to DMPK and also phosphorylates the sequence RRASV (*39*), which more closely matches the predicted DMPK phosphorylation motif. Future work involving phosphopeptide mapping of substrates phosphorylated by a larger number of DMPK family members will be critical in establishing a more detailed perspective of subfamily relationships.

Our kinetic studies indicate that the basal catalytic activity of full-length DMPK is relatively low, whereas C-terminally truncated DMPK forms exhibit an approximately 3-fold increase in V_{max}. This inhibitory activity maps within a 16 amino acid segment of the extreme C-terminus of the full-length kinase. Given the similarity of this sequence to our predicted DMPK phosphorylation motif, and the inhibition of DMPK by a peptide corresponding to this sequence, we believe that this region functions as a pseudosubstrate autoinhibitory domain, a common feature of many protein kinases (*27*).

The close relationship of DMPK to the Rho-kinases has led to speculation whether DMPK activity may be regulated in vivo by small G proteins, particularly of the Rho family. Although DMPK lacks obvious binding sites for known G

proteins, we demonstrate that DMPK isolated from cells exposed to GTP-γ-S exhibits approximately twice the activity of DMPK isolated from untreated cells. This observation is consistent with a G protein regulatory mechanism, but whether this regulation occurs via direct binding of a G protein (as with the Rho-kinases) or indirectly (possibly via intermediate kinases) remains to be determined. Future work will be directed toward the identification of these putative regulatory G proteins.

We propose a general model (Figure 12) that accounts for DMPK oligomerization, processing, and regulation. In this model, transient activation of kinase activity would occur in response to G protein second messengers, while long-term activation of DMPK could be mediated by a membrane-associated protease that cleaves DMPK-1 to release cytosolic DMPK-2 in a persistently activated form. The persistent activation of serine/threonine kinases has been shown to play a role in the in the determination of cell fate (*40*) as well as memory production in the nervous system (*41*). In this respect, DMPK may be similar to PKA and PKC, two kinases that can be transiently activated in response to second messengers or persistently activated by proteolytic removal of an autoinhibitory domain (*41*, *42*). Thus, this model suggests that the two endogenous DMPK forms may possess different activities, localizations, regulators, and substrates and perform distinct physiological functions.

REFERENCES

1. Harper, P. S. (1989) *Myotonic Dystrophy*, 2nd ed., W. B. Saunders Company, London.
2. Buxton, J., Shelbourne, P., Davies, J., Jones, C., Van Tongeren, T., Aslanidis, C., deJong, P., Jansen, G., Anvret, M., Riley, B., Williamson, R., and Johnson, K. (1992) *Nature 355*, 545−546.
3. Fu, Y.-H., Pizzuti, A., Fenwick, R. G., King, J., Rajnarayan, S., Dunne, P. W., Dubel, J., Nasser, G. A., Ashizawa, T., de Jong, P., Weiringa, B., Korneluk, R. G., Perryman, M. B., Epstein, H. F., and Caskey, C. T. (1992) *Science 255*, 1256−1258.
4. Aslandis, C., Jansen, G., Amemiya, C., Shutler, G., Mahadevan, M., Tsilfidis, C., Chen, C., Alleman, J., Wormskamp, N. G. M., Vooijs, M., Buxton, J., Johnson, K., Smeets, H. J. M., Lennon, G. G., Carrano, A. V., Korneluk, R. G., Wieringa, B., and de Jong, P. J. (1992) *Nature 355*, 548−551.
5. Mahadevan, M., Tsilfidis, C., Sabourin, L., Shutler, G., Amemiya, C., Jansen, G., Neville, C., Narang, M., Barcelo, J., O'Hoy, K., Leblond, S., Earle-Macdonald, J., deJong, P. J., Wieringa, B., and Korneluk, R. G. (1992) *Science 255*, 1253−1255.
6. Korade-Mirnics, Z., Babitzke, P., and Hoffman, E. (1998) *Nucleic Acids Res. 26*, 1363−1368.
7. Maeda, M., Taft, C. S., Bush, E. W., Holder, E., Bailey, W. M., Neville, H., Perryman, M. B., and Bies, R. D. (1995) *J. Biol. Chem. 270*, 20246−20249.
8. Whiting, E. J., Waring, J. D., Tamai, K., Somerville, M. J., Hincke, M., Staines, W. A., Ikeda, J.-E., and Korneluk, R. G. (1995) *Hum. Mol. Genet. 4*, 1063−1072.
9. Pham, Y. C., Man, N., Lam, L. T., and Morris, G. E. (1998) *Hum. Mol. Genet. 7*, 1957−65.
10. Waring, J. D., Haq, R., Tami, K., Sabourin, L. A., Ikeda, J.-E., and Korneluk. (1996) *J. Biol. Chem. 271*, 15187−15193.
11. Watson, K. L. (1995) *BioEssays 17*, 673−676.
12. Cohen, C., and Parry, D. A. D. (1990) *Proteins 7*, 1−15.
13. Roe, J. L., Durfee, T., Zupan, J. R., Repetti, P. P., McLean, B. G., and Zambryski, P. C. (1997) *J. Biol. Chem. 272*, 5838−5845.
14. Matsui, T., Amano, M., Yamamoto, T., Chihara, K., Nakafuku, M., Ito, M., Nakano, T., Okawa, K., Iwamatsu, A., and Kaibuchi, K. (1996) *EMBO J. 15*, 2208−2216.
15. Luo, L., Lee, T., Tsai, L., Tang, G., Jan, L. Y., and Jan, Y. N. (1997) *Proc. Natl. Acad. Sci. 94*, 12963−12968.
16. Leung, T., Chen, X., Tan, I., Manser, E., and Lim, L. (1998) *J. Biol. Chem. 18*, 130−140.
17. Wissman, A., Ingles, J., McGhee, J. D., and Mains, P. E. (1997) *Genes & Development 11*, 409−422.
18. Verde, F., Wiley, D. J., and Nurse, P. (1998) *Proc. Natl. Acad. Sci. U.S.A. 95*, 7526−7531.
19. Peterson, G. (1983) *Methods Enzymol. 91*, 95−119.
20. Dunne, P. W., Walch, E. T., and Epstein, H. F. (1994) *Biochemistry 33*, 10809−10814.
21. Alberti, S., Oehler, S., Wilcken-Bergmann, B. V., and Muller-Hill, B. (1993) *EMBO J. 12*, 3227−3236.
22. Kemp, B. E., Graves, D. J., Benjamini, E., and Krebs, E. G. (1977) *Journal of Biological Chemistry 252*, 4888−4894.
23. Malencik, D. A., and Anderson, S. R. (1983) *Analytical Biochemistry 132*, 34−40.
24. House, C., Wettenhall, R. E. H., and Kemp, B. E. (1987) *J. Biol. Chem 262*, 772−777.
25. Pearson, R. B., and Kemp, B. E. (1991) *Methods Enzymol. 200*, 62−81.
26. Alexander, D. R., Graves, J. D., Lucas, S. C., Cantrell, D. A., and Crumpton, M. J. (1990) *Biochem. J. 268*, 303−308.
27. Kemp, B. E., Pearson, R. B., and House, C. M. (1991) *Methods Enzymol. 201*, 287−304.
28. Cheng, H. C., Kemp, B. E., Pearson, R. B., Smith, A. J., Miscon, L., Van Patten, S. M., and Walsh, D. A. (1986) *J. Biol. Chem. 261*, 989−992.
29. House, C., and Kemp, B. E. (1990) *Cellular Signaling 2*, 187−190.
30. Eichholtz, E., de Bont, D. B. A., de Widt, J., Lisakamp, R. M. J., and Ploegh, H. L. (1993) *J. Biol. Chem. 268*, 1982−1986.
31. Smith, M. K., Colbran, R. J., and Soderling, T. R. (1990) *J. Biol. Chem. 265*, 1837−1840.
32. Chen, S.-J., Klann, E., Gower, M. C., Powell, C. M., Sessoms, J. S., and Sweatt, J. D. (1993) *Biochemistry 32*, 1032−1039.
33. Timchenko, L., Nastainczyk, W., Schneider, T., Patel, B., Hofmann, F., and Caskey, C. T. (1995) *Proc. Natl. Acad. Sci. 92*, 5366−5370.
34. Kishimoto, A., Nishiyama, K., Nakanishi, H., Uratsuji, Y., Nomura, H., Takeyama, Y., and Nishizuka, Y. (1985) *J. Biol. Chem. 260*, 12492−12499.
35. Lovejoy, B., Choe, S., Cascio, D., McRorie, D. K., DeGrado, W. F., and Eisenberg, D. (1993) *Science 259*, 1288−1293.
36. Harbury, P. B., Zhang, T., Kim, P. S., and Alber, T. (1993) *Science 262*, 1401−1407.
37. Lupas, A., Van Dyke, M., and Stock, J. (1991) *Science 252*, 1162−1164.
38. Amano, M., Ito, M., Kimura, K., Fukata, Y., Chihara, K., Nakano, T., Matsuura, Y., and Kaibuchi, K. (1996) *J. Biol. Chem. 271*, 20246−20249.
39. Zhao, Y., Loyer, P., Li, H., Valentine, V., Kidd, V., Kraft, A. S. (1997) *J. Biol. Chem. 272*, 10013.
40. Edlund, T., and Jessell, T. (1999) *Cell 96*, 211−224.
41. Schwartz, J. H. (1993) *Proc. Natl. Acad. Sci. U.S.A. 90*, 8310−8313.
42. Chain, D. G., Hegde, A. N., Yamamoto, N., Liu-Marsh, B., and Schwartz, J. H. (1995) *J. Neurosci. 15*, 7592−7603.

BI992142F